

SPECIAL
ISSUE

Novel Triazolopyrimidine-Derived Cannabinoid Receptor 2 Agonists as Potential Treatment for Inflammatory Kidney Diseases

Matthias Nettekoven,^{*[a]} Jean-Michel Adam,^[a] Stefanie Bendels,^[a] Catarina Bissantz,^[a] Jürgen Fingerle,^[b] Uwe Grether,^[a] Sabine Grüner,^[b] Wolfgang Guba,^[a] Atsushi Kimbara,^[a] Giorgio Ottaviani,^[c] Bernd Püllmann,^[a] Mark Rogers-Evans,^[a] Stephan Röver,^[a] Benno Rothenhäusler,^[c] Sebastien Schmitt,^[a] Franz Schuler,^[c] Tanja Schulz-Gasch,^[a] and Christoph Ullmer^[b]

Dedicated to Prof. Steven V. Ley on the occasion of his 70th birthday

The cannabinoid receptor 2 (CB2) system is described to modulate various pathological conditions, including inflammation and fibrosis. A series of new heterocyclic small-molecule CB2 receptor agonists were identified from a high-throughput screen. Lead optimization gave access to novel, highly potent, and selective (over CB1) triazolopyrimidine derivatives. A preliminary structure–activity relationship was established, and physicochemical properties in this compound class were significantly improved toward better solubility, lipophilicity, and microsomal stability. An optimized triazolopyrimidine derivative, (3*S*)-1-[5-*tert*-butyl-3-[(1-cyclopropyltetrazol-5-yl)methyl]triazolo[4,5-*d*]pyrimidin-7-yl]pyrrolidin-3-ol (**39**), was tested in a kidney ischemia–reperfusion model, in which it showed efficacy at a dose of 10 mg kg⁻¹ (p.o.). A significant depletion of the three measured kidney markers indicated a protective role of CB2 receptor activation toward inflammatory kidney damage. Compound **39** was also protective in a model of renal fibrosis. Oral treatment with **39** at 3 mg kg⁻¹ per day significantly decreased the amount of fibrosis by ~40% which was induced by unilateral ureter obstruction.

Several protective mechanisms in mammalian tissues have developed over the course of evolution to prevent and limit injuries caused by various types of insults. An important part of

this protective mechanism is in lipid signaling through activation of the cannabinoid 2 (CB2) receptor-mediated pathway.^[1] During the insult a rapid increase in local endocannabinoid levels causes a sudden modulation of various signaling pathways in immune and other cell types. Endocannabinoids, endocannabinoid-like, and synthetic CB2 receptor agonists positively affect a large number of pathological conditions, including cardiovascular,^[2] gastrointestinal,^[3] liver,^[4] kidney,^[5] lung,^[6] neurodegenerative^[7] and psychiatric^[8] disorders, as well as pain,^[9] cancer,^[10] bone,^[11] reproductive system,^[12] and skin pathologies.^[13] Typical endogenous CB2 receptor agonists are compounds such as anandamide (AEA)^[14] and 2-arachidonoylglycerol (2-AG),^[15] as well as plant-derived Δ^9 -tetrahydrocannabinol ((-)- Δ^9 -THC)^[14] and exogenous cannabinoid-type agonists such as HU-308,^[14] JWH-133,^[16] and HU-910.^[4] Non-cannabinoid-type agonists have been described in several recent overviews.^[17] All of these CB2 receptor agonists possess various degrees of potency and selectivity versus the cannabinoid 1 (CB1) receptor.^[18]

With the goal to identify new selective CB2 receptor agonist hit structures, a high-throughput screen was performed. Various hit clusters were identified by an automated analysis of the hit list with a combination of fingerprint and maximum common substructure methods.^[19] The analysis was based on agonistic potency at the CB2 receptor (cAMP assay) and selectivity versus the CB1 receptor (cAMP assay) within a cluster of similar compounds. A cluster with seven members of heterocyclic compounds was identified for hit evaluation and lead optimization. Four typical derivatives with their preliminary profiles are shown in Table 1.

The most potent compound from the seven members in this cluster was triazolopyrimidine **1** (IUPAC atom numbering), with an EC₅₀ value of 9 nM at the CB2 receptor as measured by cAMP assay,^[20] a full agonist in this assay with high selectivity versus CB1 (EC₅₀ > 10 μ M) in the respective cAMP assay. CB2 β -arrestin data were also determined for selected compounds.^[21] The ability of CB2 agonists to recruit β -arrestin ultimately leads to the steric inhibition of G-protein coupling and termination of signaling-independent of G-protein classes. Partial agonists might constitutively stimulate receptor activation without causing β -arrestin recruitment. This might be considered a cru-

[a] Dr. M. Nettekoven, Dr. J.-M. Adam, Dr. S. Bendels, Dr. C. Bissantz, Dr. U. Grether, Dr. W. Guba, Dr. A. Kimbara, B. Püllmann, Dr. M. Rogers-Evans, Dr. S. Röver, S. Schmitt, Dr. T. Schulz-Gasch
Roche Pharmaceutical Research and Early Development
Small-Molecule Research, Roche Innovation Center Basel
Grenzacher Str. 124, 4070 Basel (Switzerland)
E-mail: matthias.nettekoven@roche.com

[b] Dr. J. Fingerle, Dr. S. Grüner, Dr. C. Ullmer
Roche Pharmaceutical Research and Early Development
Discovery Biology, Roche Innovation Center Basel
Grenzacher Str. 124, 4070 Basel (Switzerland)

[c] Dr. G. Ottaviani, Dr. B. Rothenhäusler, Dr. F. Schuler
Roche Pharmaceutical Research and Early Development
DMPK, Roche Innovation Center Basel
Grenzacher Str. 124, 4070 Basel (Switzerland)

This article is part of a Special Issue on Drug Discovery in the Field of Autoimmune and Inflammatory Disorders. The complete issue can be browsed via Wiley Online Library.

Table 1. Four representative derivatives of a cluster identified through HTS.

| Compd: | 1 | 2 | 3 | 4 |
|---------------------------------------|-------|-------------------|-------|-------------------|
| hCB2 cAMP EC ₅₀ [μM] | 0.009 | 3.6 | 0.8 | 0.26 |
| Efficacy [%] | 100 | 100 | 73 | 77 |
| hCB1 cAMP EC ₅₀ [μM] | > 10 | > 10 | > 10 | > 10 |
| hCB2 β-arrestin EC ₅₀ [μM] | 0.08 | ND ^[a] | 0.64 | ND ^[a] |
| Efficacy [%] | 100 | ND ^[a] | 49 | 49 |
| AlogP | 4.2 | 3.85 | 4.12 | 3.5 |
| M _r [Da] | 386.9 | 310.4 | 281.4 | 315.7 |

[a] Not determined.

cial parameter for the translation of in vitro potency into in vivo efficacy.^[22] Triazolopyrimidine **1** was active with EC₅₀ = 80 nM in the human CB2 β-arrestin assay with 100% efficacy. Calculated lipophilicity (AlogP^[23]) and molecular weight values (M_r) served to determine the potential for optimization of molecular properties by diversification. Triazolopyrimidine **1** showed an AlogP value of 4.2, with M_r < 400 Da, and at least three vectors available for diversification. Close analogues **2–4** were of even lower molecular weight with similar AlogP values.^[24]

A 3D homology model of CB2 was built in MOE using the published X-ray crystal structure of activated bovine rhodopsin as a template.^[25] Compounds **1–4** were manually docked into the binding site and superimposed to rationalize the SAR within the series and to guide optimization efforts. As shown in Figure 1, substituents at positions 3 and 5 are in contact with the external loops region. The proposed binding mode in the homology models suggests that the R5 pocket should be able to accommodate small and branched linear as well as cyclic alkyl substituents. The R5 pocket is defined by aromatic and aliphatic amino acid side chains; therefore, hydrogen bond donors or acceptors are not expected to contribute beneficially to CB2 activity. The R3 pocket is predominantly hydrophobic as well; however, the pocket size is significantly larger than R5. The orthogonal orientation of delineating residues forms an aromatic box, which is optimally suited for accommodating aromatic substituents. For an optimal placement within the R3 pocket, linkers such as CH₂ are required to project aromatic cores with an exit vector of 90° in the back of the pocket. The pocket size also allows further small substituents at the R5 aromatic rings. In contrast to R3 and R5, substituents at position 7 extend downward into the transmembrane region. The volume of the pocket is sufficiently large for up to six-membered aliphatic rings. Besides the orientation of the R7 pocket deep in the transmembrane core region, this pocket also differs from R3 and R5 by two additional polar amino acids: serine and threonine. Thus, the proper placement of hydrogen bond donors or acceptors should enable the modula-

tion of physicochemical properties as well as enhancement of binding affinity. As described below, this pocket is also instrumental for optimizing selectivity toward the CB1 receptor (Figure 1).

This analysis of computational properties in combination with fitting of the compounds of this cluster into the CB2 homology model supports our confidence in this hit cluster in conjunction with CB2 functional activity, and allowed the start of a chemical optimization program. Starting with triazolopyrimidine **1**, the most active compound of this

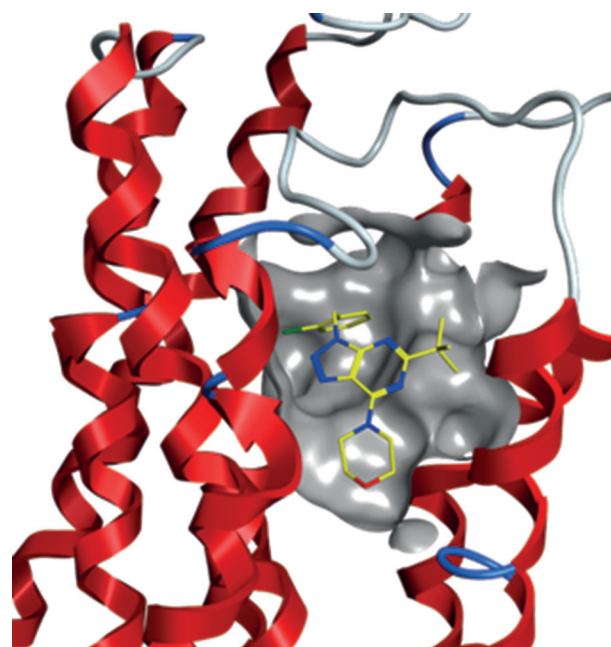
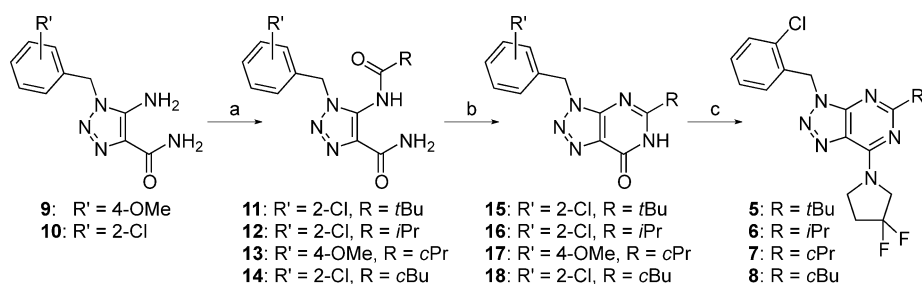


Figure 1. Manual docking of compound **1** into the binding site of the CB2 homology model. Protein residues and nonpolar hydrogen atoms of the ligand are omitted for clarity. The N-terminal loop region is located at the top.

cluster, three vectors of diversification were investigated. The nature and role of the substitution at position 5 was studied regarding its potential to influence the activation of the CB2 receptor, selectivity versus the CB1 receptor, and molecular properties. In the early optimization phase, lipophilicity (calculated with AlogP^[23]), aqueous solubility in phosphate buffer pH 6.5 (LYSA^[26]), and liver microsomal clearance (human and mouse)^[27] of tested compounds were systematically assessed to improve drug-likeness and pharmacokinetics (PK) via early ADME optimization.^[27] To decrease the lipophilicity, the aromaticity load of the final compounds was kept low by synthesiz-



Scheme 1. Synthesis of triazolopyrimidine derivatives 5–8. *Reagents and conditions:* a) for **11**: **10** + *tert*-butylcarbonyl chloride, pyridine, 80 °C, 3 h; for **12**: **10** + isopropanecarbonyl chloride, pyridine, 80 °C, 3 h; for **13**: **9** + cyclopropanecarbonyl chloride, pyridine, 80 °C, 3 h; for **14**: **10** + cyclobutanecarbonyl chloride, pyridine, 80 °C, 5 h; b) for **15**: **11** + KHCO_{3(aq)}, H₂O, reflux; for **16**: **12** + KHCO_{3(aq)}, H₂O, reflux; for **17**: **13** + KHCO_{3(aq)}, H₂O, reflux; for **18**: **14** + KHCO_{3(aq)}, H₂O, reflux; c) for **5**: **15** + POCl₃, reflux, 2. difluoropyrrolidine hydrochloride, DIPEA; for **6**: **16** + POCl₃, reflux, 2. difluoropyrrolidine hydrochloride, DIPEA; for **7**: **17** + POCl₃, reflux, 2. difluoropyrrolidine hydrochloride, 3. TFA, reflux, 4. 1-(bromomethyl)-2-chlorobenzene, DBU; for **8**: **18** + POCl₃, reflux, 2. difluoropyrrolidine hydrochloride.

ing analogues with alkyl and (substituted) cycloalkyl residues only. Initial profiling of triazolopyrimidine **1** in terms of microsomal stability revealed medium stability in human (h) and mouse (m) microsomes (CL_{int} [μL min⁻¹ kg⁻¹] (h/m): 34/62). Therefore, for initial studies of the role of the substituent at the 5-position, a generally more stable amine at the 7-position was chosen, that is, 3,3-difluoropyrrolidine. The synthesis of representative examples is shown in Scheme 1. The synthetic strategy focused on the versatility of the approach, and two pathways are exemplified. Triazoles **9** and **10**

are commercially available and can react conveniently with desired acyl chlorides under basic conditions to access intermediates **11–14** (compounds were typically used crude). Cyclization of **11–14** occurred under basic conditions to give compounds **15–18** (compounds either used crude or yields recorded between 14 and 41%). Derivatization of intermediates **15**, **16**, and **18** was carried out by chlorination with POCl₃ and subsequent nucleophilic substitution to access triazolopyrimidines **5**, **6**, and **8**, respectively. For the synthesis of triazolopyrimidine derivative **7**, intermediate **17** was first chlorinated and substituted with 3,3-difluoropyrrolidine, the 4-methoxybenzyl group of the intermediate was cleaved with trifluoroacetic acid (TFA), and subsequent derivatization with 2-chlorobenzyl bromide gave access to derivative **7** (Scheme 1).

The compounds were tested in functional CB2 and CB1 assays, and their preliminary molecular property profiles were assessed and compared with those of the parent, *tert*-butyltriazolopyrimidine derivative **5** (Table 2). Derivatives **5–8** all had nanomolar activity in the CB2 cAMP assay, similar to (**5**) or even better than (**6**, **7**, **8**) that of triazolopyrimidine **1**, whereas

only triazolopyrimidine **8** was found to retain the excellent selectivity against CB1 in the cAMP assay. The activity in the human CB2 β-arrestin assay remained very similar. Molecular properties (AlogP, LYSA) for all derivatives **5–8** were very similar, and only the human and mouse microsomal stabilities differentiated this compound set. Clearance in human and mouse microsomes increased for **6**, **7**, and **8** relative to **5** (particularly in mouse microsomes); however, compound **5** is more stable than the original triazolopyrimidine **1**, as an-

Table 2. Triazolopyrimidine derivatives 5–8 variously substituted at position 5.

| Compd: | | | | |
|--|--------|--------|--------|--------|
| hCB2 cAMP EC ₅₀ [μM] | 0.0002 | 0.005 | 0.001 | 0.001 |
| Efficacy [%] | 99 | 100 | 97 | 99 |
| hCB1 cAMP EC ₅₀ [μM] | 0.165 | 0.774 | 0.749 | > 10 |
| hCB2 β-arrestin EC ₅₀ [μM] | 0.023 | 0.011 | 0.012 | 0.015 |
| Efficacy [%] | 88 | 66 | 60 | 51 |
| AlogP | 5.08 | 4.66 | 4.29 | 4.74 |
| LYSA [μg mL ⁻¹] | < 1 | < 1 | < 1 | < 1 |
| CL _{int} [μL min ⁻¹ kg ⁻¹] (h/m) | 10/43 | 18/189 | 42/330 | 29/164 |

anticipated. This demonstrated that isopropyl, cyclopropyl, and cyclobutyl (amongst other variations at position 5; data not shown) are not viable alternatives to the originally identified *tert*-butyl group. Therefore, optimization of activities and properties of the triazolopyrimidine class was studied with the *tert*-butyl group fixed at the 5-position. The primary focus was then turned to substitution at position 7 with ethers and amines. Substitution of intermediate **15** (obtained through reaction with POCl₃) with various alcohols under basic conditions yielded a set of substituted triazolopyrimidines, of which a selection (**19–22**) of the most potent derivatives is listed in Table 3.

The compounds were tested in functional CB2 and CB1 assays, and their preliminary molecular property profiles were assessed. In general, triazolopyrimidines with an ether substitution at the 7-position were all active in the nanomolar range, displaying full efficacy toward the hCB2 receptor coupled with good selectivity versus the hCB1 receptor (EC₅₀ > 10 μM). EC₅₀ values for β-arrestin for **19–22** were found < 1 μM, with partial efficacy of ~70%. For these most potent derivatives, AlogP

Table 3. Triazolopyrimidine derivatives **19–22** substituted with ethers at position 7.

| Compd: | 19 | 20 | 21 | 22 |
|--|-----------|-----------|-----------|-----------|
| hCB2 cAMP EC ₅₀ [μM] | 0.017 | 0.01 | 0.008 | 0.022 |
| Efficacy [%] | 97 | 98 | 97 | 98 |
| hCB1 cAMP EC ₅₀ [μM] | > 10 | > 10 | > 10 | > 10 |
| hCB2 β-arrestin EC ₅₀ [μM] | 0.31 | 0.349 | 0.746 | 0.61 |
| Efficacy [%] | 61 | 61 | 72 | 72 |
| AlogP | 5.15 | 5.06 | 5.72 | 5.74 |
| LYSA [μg mL ⁻¹] | < 11 | < 1 | < 1 | < 1 |
| CL _{int} [μL min ⁻¹ kg ⁻¹] (h/m) | 15/703 | 140/1000 | 14/149 | 60/303 |

values were not improved and were calculated to be > 5. They subsequently showed low aqueous solubility (LYSA: < 1 μg mL⁻¹). The microsomal clearance in human and mouse microsomes was higher than the nitrogen-substituted triazolopyrimidine **5** (cf. Table 2), and therefore optimization of the ether derivatives was not pursued further.

Optimization of activities and properties of the triazolopyrimidines was studied with a wide selection of amines at the 7-position. Substitution of intermediate **15** (as before) with various amines under basic conditions yielded a set of substituted triazolopyrimidines, of which a selection is shown in Table 4 which serve to illustrate the emerging SAR. Triazolopyrimidines substituted at the 7-position with primary amines (i.e., **23** and **24**) generally yielded compounds active at the CB2 receptor in the nanomolar range (**23**, EC₅₀ = 0.011 μM); however, depending on the size of the substituent, significantly less active (**24**, EC₅₀ = 0.647 μM) with very good selectivity versus the CB1 receptor (EC₅₀ > 10 μM). Molecular properties of such derivatives were very similar, with AlogP values > 5, mainly with low solubility and generally high microsomal clearance values. Triazolopyrimidines substituted with aliphatic secondary amines (i.e., **25**) displayed a very similar profile in terms of activities and

generally 10-fold less active. Activity at the CB1 receptor for these derivatives was also affected. Derivatives **26–28** showed activity in the high-nanomolar/low-micromolar range. The selectivity against the CB1 receptor remains very high (e.g., the ratio [hCB1 cAMP EC₅₀]/[hCB2 cAMP EC₅₀] for **27** is > 2100).

β-Arrestin values were measured only for derivatives **26** and **27**, and for both compounds activities of ~100 nM with partial efficacy (~76%) were observed. The molecular properties of these compounds were not significantly improved, with one main issue being high clearance in human and mouse microsomes. Nevertheless, the significant improvement in CB2 activity with the pyrrolidine-substituted triazolopyrimidine **27** (as also previously observed with triazolopyrimidine **5** with a 3,3-difluoropyrrolidine group at the 7-position) led to an investigation of the influence of substituted pyrrolidine derivatives on activity/selectivity and molecular properties. Synthetic access to such derivatives was identical to that described above: that is, substitution of core intermediate **18** with various substituted pyrrolidines. A selection of these derivatives is shown in Table 5 to illustrate the general effects.

2-Substituted pyrrolidine triazolopyrimidines (i.e., **29**) were generally weaker in terms of potency at the CB2 receptor and metabolically weaker than their isomeric 3-substituted pyrrolidine triazolopyrimidine counterparts (i.e., **30**), although still active in the low-nanomolar range. Although selectivity versus the CB1 receptor for the 2-substituted pyrrolidine triazolopyrimidine derivatives could be influenced, no general trend was deduced. Alkyl substitution (at the 2- or 3-positions) led to compounds with β-arrestin values in the higher nanomolar range with partial or full efficacy. Substitution of the pyrrolidine ring with one fluorine atom at the 3-position led to triazolopyr-

Table 4. Selection of triazolopyrimidine derivatives **23–28** substituted with amines at position 7.

| Compd: | 23 | 24 | 25 | 26 | 27 | 28 |
|--|-------------------|-------------------|-------------------|-----------|-----------|-------------------|
| hCB2 cAMP EC ₅₀ [μM] | 0.011 | 0.647 | 0.017 | 0.003 | 0.0003 | 0.0016 |
| Efficacy [%] | 98 | 90 | 98 | 100 | 100 | 100 |
| hCB1 cAMP EC ₅₀ [μM] | > 10 | > 10 | > 10 | 1.0 | 0.631 | 0.555 |
| hCB2: β-arrestin EC ₅₀ [μM] | ND ^[a] | ND ^[a] | ND ^[a] | 0.09 | 0.132 | ND ^[a] |
| Efficacy [%] | ND ^[a] | ND ^[a] | ND ^[a] | 75 | 78 | ND ^[a] |
| AlogP | 4.51 | 6.02 | 5.21 | 4.39 | 4.97 | 5.43 |
| LYSA [μg mL ⁻¹] | < 1 | ND ^[a] | < 1 | < 1 | < 1 | < 1 |
| CL _{int} [μL min ⁻¹ kg ⁻¹] (h/m) | 103/915 | ND ^[a] | 37/287 | 46/324 | 76/256 | 45/154 |

[a] Not determined.

Table 5. Selection of triazolopyrimidine derivatives **29–34** carrying substituted pyrrolidines at position 7.

| Compd: | 29 | 30 | 31 | 32 | 33 | 34 |
|--|-----------|-----------|-----------|-----------|-----------|-----------|
| hCB2 cAMP EC ₅₀ [μM] | 0.026 | 0.013 | 0.0005 | 0.0006 | 0.0003 | 0.003 |
| Efficacy [%] | 100 | 101 | 101 | 101 | 101 | 101 |
| hCB1 cAMP EC ₅₀ [μM] | > 100 | 1.7 | 0.432 | > 10 | 0.491 | > 10 |
| hCB2 β-arrestin EC ₅₀ [μM] | 0.93 | 0.321 | 0.071 | 0.031 | 0.023 | 0.102 |
| Efficacy [%] | 65 | 86 | 85 | 114 | 106 | 106 |
| Alog <i>P</i> | 5.35 | 5.29 | 4.82 | 3.88 | 4.46 | 3.37 |
| LYSA [μg mL ⁻¹] | < 1 | < 1 | < 1 | < 1 | < 1 | 7 |
| CL _{int} [μL min ⁻¹ kg ⁻¹] (h/m) | 44/263 | 25/63 | 16/59 | 10/43 | 25/166 | 10/27 |

imidine **31**, which is active at the CB2 receptor in the sub-nanomolar range and active versus the CB1 receptor in the sub-micromolar range. β-Arrestin values remained in the higher nanomolar range with partial efficacy. Substitution of the pyrrolidine ring at the 3-position generally led to compounds (i.e., **30**, **31**, and **32**) with medium to low clearance values in human and mouse microsomes. This was also already anticipated and observed with compound **5**. Solubility remained low for the three compounds; lipophilicity, however, could be decreased from Alog*P*=5.08 (**5**) to Alog*P*=3.88 for compound **32**.

A comparative analysis of the CB1 and CB2 binding pockets of the homology models revealed that the substituent at position 7 is deeply buried and is in close proximity to Phe199 in CB1. The corresponding residue in CB2 is Ser193. This difference in the sub-pocket for the 7-position substituent suggests the attachment of a hydroxy group to the pyrrolidine ring, which would be able to form a hydrogen bond to the Ser193 side chain in CB2 (Figure 2). The expectation was to introduce more polarity into the molecule and to improve its selectivity for CB1. The Phe199 side chain in CB1 is sterically more demanding than the corresponding Ser193 residue in CB2; moreover, it cannot form a hydrogen bond with the hydroxy group of the ligand.

Indeed, derivative **32**, with an unprotected hydroxy group on the pyrrolidine ring, was found to have activity at the CB2 receptor in the sub-nanomolar range, and remarkably, this compound has greater than 10000-fold selectivity versus the CB1 receptor and a β-arrestin value of 32 nm with full efficacy. Furthermore, the lipophilicity could be decreased (Alog*P*: 3.88). The solubility, however, remained low. Stability in microsomes was observed to be in the same range as for compounds **30** and **31**, and an initial concern that the free hydroxy group might give rise to an alternate clearance mechanism through hepatocytes was not fully substantiated, as the compound was cleared in human and mouse hepatocytes as well with medium clearance values (data not shown). 2-(Hydroxymethyl)pyrrolidine derivative **33** was active as well at the CB2 receptor in the sub-nanomolar range, and active at the CB1 receptor with an EC₅₀ value of 0.491 μM, with a β-arrestin value

of 23 nm and full efficacy. Lipophilicity remained above 4 and solubility low. Microsomal clearance was also influenced unfavorably. Disubstituted pyrrolidine **34** was also active toward the CB2 receptor in the sub-nanomolar range, selective versus the CB1 receptor, and potent and efficacious in the CB2 β-arrestin assay. The lipophilicity of **34** was decreased to Alog*P* 3.37, and the solubility was enhanced slightly to 7 μg mL⁻¹; however, the compound was even less stable in human microsomes. In

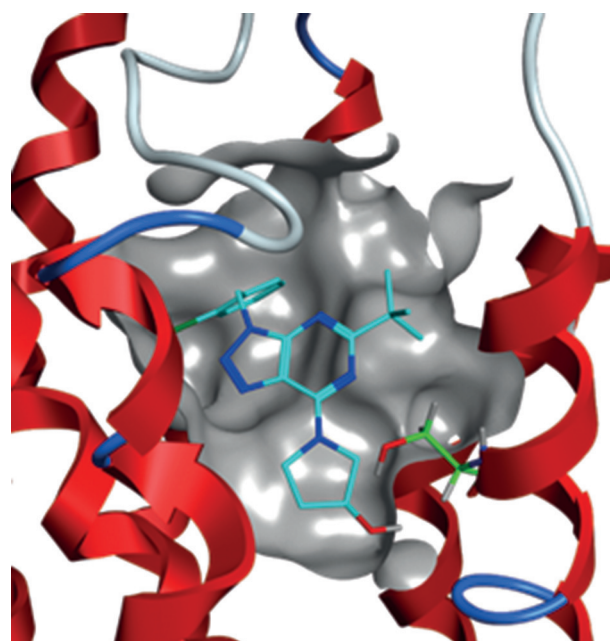
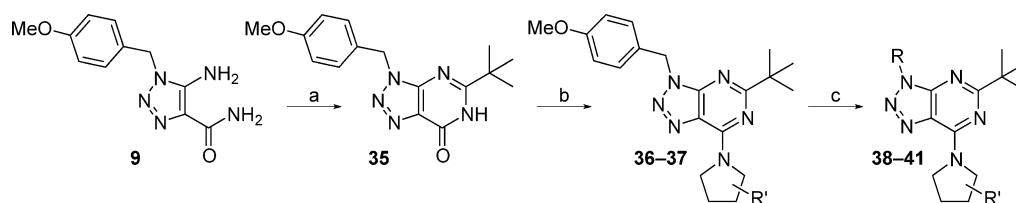


Figure 2. Compound **32** with a hydroxylated pyrrolidine at position 7 within the CB2 homology model. The OH group is postulated to form a hydrogen bond with Ser193. The corresponding residue in CB1 is Phe199 (not shown), which disfavors the binding of the hydroxylated substituents at position 7.

summary, appropriate substitution of the pyrrolidine ring yielded very potent compounds at the CB2 receptor, some with remarkably high selectivity versus the CB1 receptor. The molecular properties could be influenced to yield compounds with some solubility, lipophilicity at ~3, with medium to low microsomal clearance.

With these encouraging results we turned our attention to optimization of the substituent at the 3-position with the goal of maintaining potency toward CB2 and selectivity versus CB1 and improving properties of lipophilicity, solubility, and stability even further. Synthetic access followed the same principle as detailed previously; this is shown in Scheme 2. 5-Amino-1-(4-methoxybenzyl)-1*H*-1,2,3-triazole-4-carboxamide **9** was allowed to react with pivaloyl chloride in pyridine to access the



Scheme 2. Synthesis of triazolopyrimidine derivatives **38–41**. *Reagents and conditions:* **39**: a) **1**. **9** + pivaloyl chloride, pyridine, 80 °C, 3 h, 2. $\text{KHCO}_3(\text{aq})$, H_2O , reflux (35% over two steps); b) 1. **35** + POCl_3 , reflux, 2. (S)-pyrrolidin-3-ol, DIPEA, CH_3CN , RT (88% over two steps); c) **36** + Et_3SiH , TFA, 70 °C, 22 h, 2. 5-(chloromethyl)-1-cyclopropyl-1H-tetrazole, DBU, DMF, 3. CH_3OH (40% over three steps).

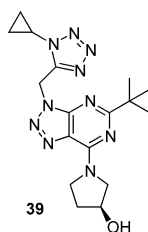
respective pivalamide, which cyclized under aqueous basic conditions to give triazolopyrimidine **35** in 35% yield over two steps. Subsequent chlorination of **35** with POCl_3 yielded the building block for derivatization with various amines at the 7-position. To access precursors for the final (S)-3-hydroxypyrrolidine-substituted triazolopyrimidines **38** and **39**, the chlorinated intermediate was reacted with 3-(S)-hydroxypyrrolidine to yield intermediate **36**. Cleavage of the 4-methoxybenzyl protecting group at position 3 from **36** was accomplished with triethylsilane and TFA, during which the free hydroxy group was trifluoroacetylated. This approach was deemed convenient, as derivatization at the 3-position was achieved by reaction with electrophiles under strong basic conditions without the free hydroxy group leading to undesired byproducts. Final cleavage of the trifluoroacetyl ester was carried out with methanol during the workup procedure to obtain compounds **38** and **39**. Similarly, the chlorinated precursor was reacted with 3,3-difluoropyrrolidine to access intermediate **37**, the PMB group again was removed with triethylsilane/TFA, and derivatization was performed with electrophiles under basic conditions to access triazolopyrimidine derivatives **40** and **41**. The compounds were tested in CB2 and CB1 receptor assays, and their initial profiles regarding lipophilicity, solubility, and stability were determined. The compounds are shown in Table 6.

Substitution at the triazolopyrimidine 3-position was carried out with (substituted) alkyl and cycloalkyl groups, which generally yielded compounds inactive at the CB2 receptor. The potencies of derivatives with *meta*- or *para*-substituted benzylic groups were usually in the micromolar range. Benzylic groups with appropriate *ortho* substitution (generally electron-withdrawing groups), however, were found to be very potent. Derivatization with five-membered aromatic heterocycles with various substitution patterns yielded the most potent and interesting compounds. The combination of (S)-3-pyrrolidine substitution at the 7-position with a 2-methylsulfonylbenzyl substituent at the 3-position yielded triazolopyrimidine **38**. This compound was found to be active in the subnanomolar range with selectivity

versus CB1 of > 1000; however, the compound was still active at the CB1 receptor at 1.14 μM . The compound was active in the hCB2 β -arrestin test, with 4.7 nM and full efficacy. Remarkably, the $\text{Alog}P$ was 2.74 with a solubility of 21 $\mu\text{g mL}^{-1}$ and low metabolic clearance ($\text{CL}_{\text{int}} [\mu\text{L min}^{-1} \text{kg}^{-1}]$ (h/m): 10/36) in human and mouse microsomes, respectively. There is a 10-fold decrease in potency for the CB2 receptor in combining the (S)-3-pyrrolidine substituent at the 7-position with a benzylic tetrazole at the 3-position of triazolopyrimidine **39** relative to **38**; however, the selectivity versus CB1 is enhanced, with $\text{EC}_{50} > 10 \mu\text{M}$ (β -arrestin $\text{EC}_{50} = 22 \text{ nM}$ (119% efficacy)). Tetrazole **39** has a remarkably decreased $\text{Alog}P$ of 1.21 combined with a solubility of 162 $\mu\text{g mL}^{-1}$ and low human and mouse microsomal clearance. Substituting the triazolopyrimidine core with 3,3-difluoropyrrolidine at the 7-position generally yielded very potent compounds (i.e., **40** and **41**) toward the CB2 receptor, with excellent selectivities versus the CB1 receptor, very good potency on β -arrestin with full efficacy and decent lipophilicity in terms of $\text{Alog}P$ (4.41 and 2.24, respectively). The solubility for **40** was poor, as anticipated with the $\text{Alog}P$ value of 4.14 in comparison with (S)-3-hydroxypyrrolidine-derived triazolopyrimidines; however, human and mouse microsomal stability could be retained (**40** $\text{CL}_{\text{int}} [\mu\text{L min}^{-1} \text{kg}^{-1}]$ (h/m): 10/41; **41** $\text{CL}_{\text{int}} [\mu\text{L min}^{-1} \text{kg}^{-1}]$ (h/m): 10/42). As triazolopyrimidine **39** showed one of the most balanced profiles in terms of potency, selectivity, and in vitro ADME, it was further characterized in vivo in mouse PK studies, and the data are listed in Table 7.

Table 6. Selection of triazolopyrimidine derivatives **38–41** substituted at position 3.

| Compd: | 38 | 39 | 40 | 41 |
|--|-----------|-----------|-----------|-----------|
| hCB2 cAMP EC_{50} [μM] | 0.0001 | 0.0007 | 0.00007 | 0.0005 |
| Efficacy [%] | 100 | 102 | 103 | 100 |
| hCB1 cAMP EC_{50} [μM] | 1.41 | > 10 | 0.098 | > 10 |
| hCB2 β -arrestin EC_{50} [μM] | 0.0047 | 0.022 | 0.0041 | 0.021 |
| Efficacy [%] | 110 | 119 | 86 | 122 |
| $\text{Alog}P$ | 2.74 | 1.21 | 4.14 | 2.24 |
| LYSA [$\mu\text{g mL}^{-1}$] | 21 | 162 | < 1 | 32 |
| $\text{CL}_{\text{int}} [\mu\text{L min}^{-1} \text{kg}^{-1}]$ (h/m) | 10/63 | 10/71 | 10/41 | 10/42 |

Table 7. Physicochemical and early safety profile of triazolopyrimidine **39**.

| | |
|--|----------------------------|
| CB2 cAMP EC ₅₀ [μM] (h/m) | 0.007/0.004 |
| Efficacy [%] (h/m) | 103/101 |
| M _r [Da] | 384 |
| PAMPA P _{eff} [10 ⁻⁶ cm s ⁻¹] | 3 (8/30/62) ^[a] |
| Microsomal CL _{int} [μL min ⁻¹ kg ⁻¹] (h/m/rat) | 10/71/143 |
| In vivo mouse CL [μL min ⁻¹ kg ⁻¹] | 37 |
| PPB (fu) [%] ^[b] (h/m) | 13.2/3.1 |
| GSH (human liver microsomes) adducts | none detected |
| CYP reversible inhibition [μM] (3A4/2C9/2D6) | > 50/16/> 50 |
| CB2 K _i [μM] (h/m) | 0.008/0.021 |
| K _i ratio hCB1/hCB2 | > 1190 |
| clog P | 0.8 (log D: 2.8) |
| H ₂ O solubility/FaSSIF/FeSSIF [μg mL ⁻¹] | 56/80/237 |
| Hepatocytes CL [mL min ⁻¹ (10 ⁶ cells) ⁻¹] (h/m) | 15/141 |
| mouse V _{ss} [L kg ⁻¹] / t _{1/2} [h] | 1.0 / 0.3 (i.v.) |
| P-gp ER ^[c] (h/m) | 6.1/19.1 |
| hERG IC ₅₀ [μM] | > 20 |
| Stability in aq. media at pH 1–10 | stable |

[a] Acceptor compartment/membrane/donor compartment (%).
[b] Plasma protein binding, fraction unbound. [c] P-glycoprotein efflux ratio.

Triazolopyrimidine **39** was equally potent toward the human and mouse CB2 receptor isoforms in the sub-nanomolar range. In a binding assay^[28] the compound was also active in the nanomolar range on the human and mouse CB2 isoforms. Here as well, the selectivity in binding versus the CB1 receptor was very high (> 1190-fold). Compound **39** has a molecular weight of 384 Da and a clog *P* of 0.8 with a measured log *D* of 2.8. The clog *P* value is in agreement with the Alog *P* value (1.21), which was used as a reference value throughout the optimization process.

Table 7 shows that passive permeability measured by PAMPA^[29] is good, as is the solubility in aqueous buffer^[30] and biologically relevant media (FaSSIF and FeSSIF).^[31] Therefore, we could expect that overall, compound **39** has a good permeability and solubility profile, and thus we anticipate good oral bioavailability. Compound **39** is not extensively bound to plasma protein, with a fraction unbound (fu) of 13.2% in human and 3.1% in mouse.^[32] It also has a high efflux ratio (ER) as measured in the P-glycoprotein transporter assay,^[33] which makes the compound potentially suitable for peripheral disease indications. Furthermore, triazolopyrimidine **39** does not inhibit the hERG channel and has a low potential to form reactive metabolites.^[34] Compound **39** also does not inhibit cytochrome P450 (CYP),^[35] and is chemically stable in the pH range of 1–10. After single i.v. dosing at 1 mg kg⁻¹ in mouse, **39** also demonstrated a good PK profile, with a moderate clearance rate (37 μL min⁻¹ kg⁻¹), a moderate volume of distri-

bution (V_{ss}: 1 L kg⁻¹), and terminal half-life of 0.3 h. Data from the mouse PK study showed triazolopyrimidine **39** to reach a concentration of 49 ng mL⁻¹ 1 h after i.v. application in plasma, which corresponds to a free concentration 10-fold above the measured mouse cAMP EC₅₀ value. This overall profile was found suitable for in vivo potency assessment. The mouse kidney ischemia–reperfusion model is used widely to access acute kidney injury (AKI).^[36] In this protocol a test compound is given to a cohort of mice at a certain concentration via gavage 30 min prior to surgery, in which the blood flow to the kidneys is stopped by firm clamping of the kidney vessels for 25 min. The resulting ischemia and subsequent reperfusion caused kidney damage, which could be ameliorated upon administration of the CB2 agonist. The level of damage and its prevention by CB2 agonists was assessed by using several readouts 24 h after ischemia–reperfusion (I/R). As direct markers of damage, plasma creatinine and urea levels were determined. Additionally, the plasma levels of three kidney biomarkers (NGAL, KIM1, and osteopontin) were analyzed at the same time point.^[37] The effect on these kidney markers upon administration of triazolopyrimidine **39** at 10 mg kg⁻¹ given orally are shown in Figure 3.

The two main readouts, creatinine and urea levels, measured 24 h after I/R showed significant decreases of ~50 and ~40%, respectively, at a dose of 10 mg kg⁻¹ after oral administration. The three biomarkers NGAL, KIM1, and osteopontin, indicative of kidney health,^[37] were also measured 24 h post-I/R. NGAL and osteopontin concentrations were significantly decreased by ~75 and ~85%, respectively. KIM1, although visibly reduced, failed to show significance due to high variability. These data clearly demonstrate that the CB2 agonist **39** has protective function, as shown by the results of the I/R experiment. Owing to the severely diseased conditions of the animals, plasma samples could not be taken during the 24 h course of the experiment. From other experiments, however (UUO; see below), in vivo PK as well as hepatocyte clearance rates could be obtained. These data suggest that high receptor occupancies are likely, especially during the critical initial phase of the experiment.

Test compound was subjected to the kidney fibrosis unilateral ureter obstruction (UUO) model, in which the ureter from one kidney is surgically ligated to cause pressure injury due to the blocked urine outflow over the course of one week.^[38] The backpressure of urine in the left kidney results in atrophy and fibrosis, as the kidney size is limited by a rigid capsule. After UUO surgery, triazolopyrimidine **39** was given orally for seven days via food admix at a dose of 3 mg kg⁻¹ per day. At the end of the experiment the kidney was perfused fixed for immunohistochemical determination of collagen-I deposition in longitudinal paraffin sections. The relative content of tissue collagen-I was determined morphometrically. The CB2 agonist induced a decrease in collagen-I deposition relative to placebo-treated animals (Figure 4). Interestingly this inhibition is in the range of inhibition of fibrosis described for angiotensin-converting enzyme (ACE) inhibitors.^[39] In our own UUO experiments, enalapril (32 mg kg⁻¹ per day in drinking water) inhibited fibrosis by 20, 43, and 54% versus placebo (UUO kidneys in

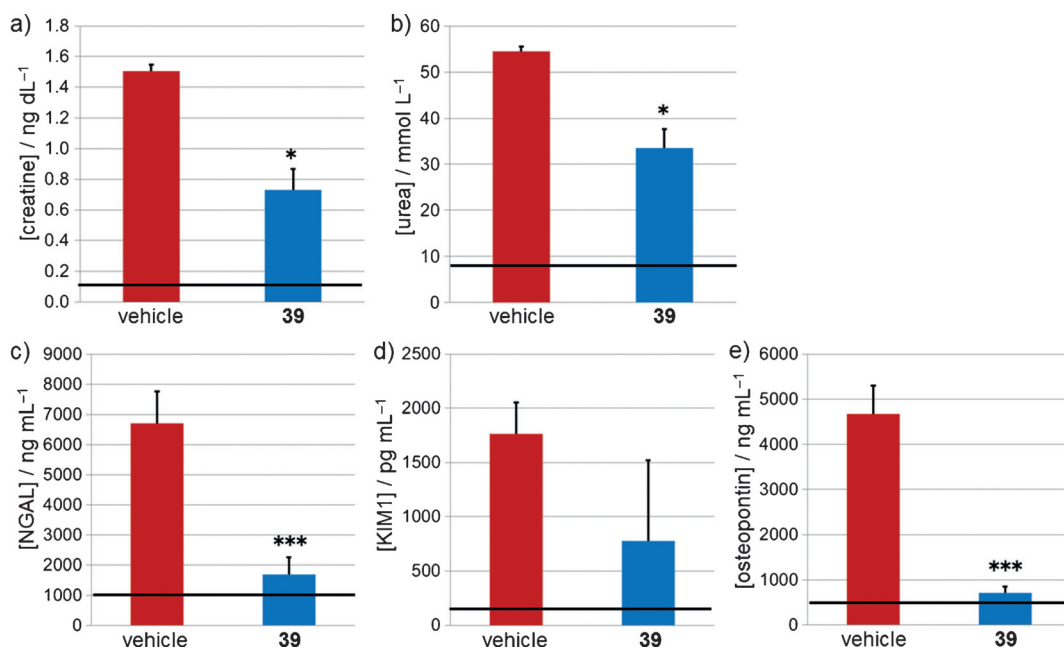


Figure 3. Results from experiments with triazolopyrimidine **39** (10 mg kg^{-1} p.o.) to show decreases in the extent of kidney injury 24 h post-I/R using readouts for: a) plasma creatinine, b) plasma urea, c) NGAL, d) KIM1, and e) osteopontin. Data are the mean \pm SD for $n=6$ independent experiments; Student's *t*-test: * $p < 0.05$, *** $p > 0.001$; KIM1 failed to reach statistical significance at $p = 0.06$. Black horizontal lines indicate sham operated animals without ligating the ureter.

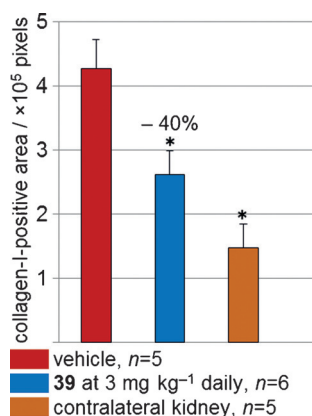


Figure 4. Results from triazolopyrimidine **39** in the UUO model.

three independent experiments with $n=6$, $p < 0.05$, Student's *t*-test).

To monitor exposure, plasma samples were collected at three time points (170 h, day 7: 21 ng mL^{-1} ; 176 h, day 7: 17 ng mL^{-1} ; 192 h, day 8: 14 ng mL^{-1}). Similar plasma concentrations were achieved at days 7 and 8, indicating that steady-state conditions were likely established. The average free plasma concentration was found to be 0.54 ng mL^{-1} , which corresponds to high receptor occupancy (e.g., 74% based on mouse cAMP data), thereby suggesting that the observed in vivo efficacy is mediated by CB2.

Immunohistochemical (IHC) analysis of collagen-I deposition in the UUO model seven days after ureter ligation of the kidney was used to determine the amount of fibrosis (colla-

gen-I). From 10 microscopic fields of each kidney, the collagen-I-positive pixel counts were determined in the cortex of each kidney. As the total area analyzed was identical for all kidneys under investigation, the absolute number of pixels was used as the relevant readout. The untreated (but ligated) vehicle kidneys show a large increase in collagen-I deposition ($n=5$, red bar) over unligated contralateral kidneys ($n=5$, orange bar). Oral treatment with triazolopyrimidine **39** at 3 mg kg^{-1} per day decreased the amount of fibrosis by $\sim 40\%$ ($n=6$, blue bar) significantly (one-way ANOVA, $p < 0.05$).

In summary, starting from an HTS campaign for the identification of potent and selective small-molecule CB2 agonists, several interesting hit clusters and single molecules were identified. The triazolopyrimidine cluster attracted our attention, as potent derivatives with SAR were identified. An extensive lead-optimization campaign in which three vectors were very systematically balanced led to the identification of preliminarily optimal substitution patterns. Thus, molecular design resulted in various highly potent CB2 agonists with excellent selectivities versus the CB1 receptor. The molecular properties could be modulated to achieve reasonable to very good solubility, lipophilicity, and stability parameters in human and mouse microsomes. The most promising triazolopyrimidines were further characterized, and compound **39** was identified as having one of the most balanced property profiles of all the compounds examined. Subsequent submission to the ischemia-reperfusion mouse model showed efficacy at a dose of 10 mg kg^{-1} p.o. in addition to the three kidney markers, which measured a significant depletion effect, thus indicating a protective potential toward inflammatory kidney damage. Triazolopyrimidine **39** was also efficacious in a model of renal fibrosis (unilateral

ureter obstruction model) at 3 mg kg⁻¹ per day. Further investigations into the triazolopyrimidine class to arrive at compounds with even higher potency and improved molecular properties that would permit reduced dosing in any given and relevant animal model are currently being pursued.

Experimental Section

Chemicals were purchased from commercial sources and were used without further purification. Reactions were magnetically and mechanically stirred and monitored by thin-layer chromatography (TLC) on Merck silica gel 60 F₂₅₄ TLC glass plates (visualized by UV fluorescence at $\lambda=254$ nm) or analytical HPLC–MS on an Agilent 1100 instrument, Finnigan single-quadrupole ESI, autosampler Gilson 215, Chromeleon 6.7, rapid resolution cartridge Zorbax XDB 3.5 μm (21 \times 30 mm). The purity of new compounds was > 95%, as determined by ¹H NMR spectroscopy after purification. Flash column chromatography was performed with silica cartridges from Silicycle, eluting with distilled technical-grade solvents on a Combi-Flash RF column. Yields refer to purified compounds. Preparative HPLC purification was carried out on a reversed-phase Phenomenex Gemini 5 mm NX-C₁₈ column, 75 \times 30 mm, AXIA, eluting with a gradient composed of CH₃CN, H₂O, and HCO₂H. NMR data were recorded on a Bruker spectrometer operating at 300, 400, and 600 MHz. Chemical shifts (δ) are reported in ppm with TMS as internal standard. The data are reported as: s=singlet, d=doublet, t=triplet, m=multiplet, br=broad signal, and coupling constant(s) *J* in Hz. Service measurements were performed by the NMR or MS service teams at F. Hoffmann–La Roche, Basel.

5-tert-Butyl-3-(2-chlorobenzyl)-7-(3,3-difluoropyrrolidin-1-yl)-3H-[1,2,3]triazolo[4,5-d]pyrimidine (5)

a) Synthesis of 15: A mixture of 5-amino-1-(2-chlorobenzyl)-1H-1,2,3-triazole-4-carboxamide (2 g, 7.95 mmol, commercially available) and pivaloyl chloride (1.47 mL, 11.9 mmol) in pyridine (3.98 mL) was stirred at 80 °C for 2 h under N₂ atmosphere. Aqueous NaOH (8 M, 2.98 mL, 23.8 mmol) and CH₃OH (3.98 mL) were then added to the reaction mixture. After stirring at 80 °C for 2 h, the reaction mixture was poured into aqueous 1 M HCl, extracted with Et₂O, washed with 2 M HCl, H₂O, and brine, dried over Na₂SO₄, and concentrated in vacuo to afford the mixture of crude 1-(2-chlorobenzyl)-5-pivalamido-1H-1,2,3-triazole-4-carboxamide and *N*-(1-(2-chlorobenzyl)-4-cyano-1H-1,2,3-triazol-5-yl)pivalamide. The residue was used for the next reaction without further purification. A mixture of the above crude residue and KHCO₃ (3.00 g, 30.0 mmol) in H₂O (60.0 mL) was held at reflux for 18 h. The reaction mixture was poured into aqueous 1 M HCl, extracted with EtOAc, washed with brine, dried over Na₂SO₄, and concentrated in vacuo. The crude residue was purified by flash chromatography (silica gel, 10 \rightarrow 70% EtOAc in heptane) to afford 5-tert-butyl-3-(2-chlorobenzyl)-3H-[1,2,3]triazolo[4,5-d]pyrimidin-7(4H)-one (15) as a white solid (1.03 g, 41% for two steps). MS (*m/z*): 318.2 [*M* + *H*]⁺; ¹H NMR (300 MHz, [D₆]DMSO): δ = 12.20 (brs, 1H), 7.08–7.61 (m, 4H), 5.73 (s, 2H), 1.29 ppm (s, 9H).

b) Synthesis of 5: A mixture of 5-tert-butyl-3-(2-chlorobenzyl)-3H-[1,2,3]triazolo[4,5-d]pyrimidin-7(4H)-one (15) (12.3 mg, 38.7 μmol) and *N,N*-diethylaniline (12.3 μL , 77.4 μmol) in POCl₃ (250 μL , 2.73 mmol) was held at reflux for 3 h under N₂ atmosphere. The reaction mixture was concentrated in vacuo, diluted with EtOAc, washed with cold H₂O and brine, dried over Na₂SO₄, and concentrated in vacuo to afford crude 5-tert-butyl-7-chloro-3-(2-chloroben-

zyl)-3H-[1,2,3]triazolo[4,5-d]pyrimidine. The residue was used for the next reaction step without further purification. A mixture of 5-tert-butyl-7-chloro-3-(2-chlorobenzyl)-3H-[1,2,3]triazolo[4,5-d]pyrimidine (crude, 47.2 μmol), 3,3-difluoropyrrolidine hydrochloride (13.6 mg, 94.4 μmol), and *N,N*-diisopropylethylamine (DIPEA; 12.2 mg, 94.4 μmol) in CH₃CN (250 μL) was stirred at room temperature overnight. The reaction mixture was directly purified by preparative HPLC [column: Gemini 5 μm C₁₈ 110A 75 \times 30 mm; mobile phase: (0.05% HCO₂H in H₂O)/CH₃CN 40:60 \rightarrow 5:95 v/v gradient over 8 min; λ = 280 nm; flow rate: 30 mL min⁻¹] to afford 5-tert-butyl-3-(2-chlorobenzyl)-7-(3,3-difluoropyrrolidin-1-yl)-3H-[1,2,3]triazolo[4,5-d]pyrimidine (5) as a colorless gum (13.3 mg, 69% for two steps). MS (*m/z*): 407.7 [*M* + *H*]⁺; ¹H NMR (300 MHz, CDCl₃): δ = 7.34–7.46 (m, 1H), 7.16–7.26 (m, 3H), 5.88 (s, 2H), 4.40–4.78 (m, 2H), 3.91–4.29 (m, 2H), 2.33–2.74 (m, 2H), 1.34 ppm (s, 9H).

(3S)-1-[5-tert-Butyl-3-[(1-cyclopropyltetrazol-5-yl)methyl]triazolo[4,5-d]pyrimidin-7-yl]pyrrolidin-3-ol (39)

a) Synthesis of 35: A mixture of 5-amino-1-(4-methoxybenzyl)-1H-1,2,3-triazole-4-carboxamide 9 (10.0 g, 10 mmol) and pivaloyl chloride (7.47 mL, 60.7 mmol) in pyridine (20.2 mL) was stirred at 80 °C for 2 h under N₂ atmosphere. Aqueous NaOH (8 M, 15.2 mL, 121 mmol) and CH₃OH (20.2 mL) were then added to the reaction mixture. After stirring at 80 °C for 1 h, the reaction mixture was poured into aqueous 1 M HCl, extracted with Et₂O, washed with aqueous 2 M HCl, H₂O and brine, dried over Na₂SO₄, and concentrated in vacuo to afford the mixture of crude 1-(4-methoxybenzyl)-5-pivalamido-1H-1,2,3-triazole-4-carboxamide and *N*-(4-cyano-1-(4-methoxybenzyl)-1H-1,2,3-triazol-5-yl)pivalamide. The residue was used for the next reaction without further purification. A mixture of the above crude residue and KHCO₃ (12.1 g, 121 mmol) in H₂O (242 mL) was held at reflux for 18 h. The reaction mixture was poured into aqueous 1 M HCl, extracted with EtOAc, washed with brine, dried over Na₂SO₄, and concentrated in vacuo. The crude residue was purified by flash chromatography (silica gel, 10 \rightarrow 70% EtOAc in heptane) to afford 5-tert-butyl-3-(4-methoxybenzyl)-3H-[1,2,3]triazolo[4,5-d]pyrimidin-7(4H)-one (35) (4.44 g, 35% for two steps). MS (*m/z*): 314.2 [*M* + *H*]⁺.

b) Synthesis of 36: 5-tert-Butyl-3-(4-methoxybenzyl)-3H-[1,2,3]triazolo[4,5-d]pyrimidin-7(4H)-one (35) (255 mg, 814 μmol), POCl₃ (5.03 g, 3.0 mL, 32.8 mmol), and *N,N*-diethylaniline (243 mg, 259 μL , 1.63 mmol) were combined in a 5-mL vessel to give a light-yellow solution. The reaction mixture was heated at 120 °C and stirred for 4 h. The crude reaction mixture was concentrated in vacuo and poured into 1 mL H₂O and extracted with EtOAc (2 \times 2 mL). The organic layers were combined, washed with saturated aqueous NaCl (1 \times 1 mL), dried over Na₂SO₄, and concentrated in vacuo to yield 5-tert-butyl-7-chloro-3-(4-methoxybenzyl)-3H-[1,2,3]triazolo[4,5-d]pyrimidine, which was used crude in the subsequent reaction. 5-tert-Butyl-7-chloro-3-(4-methoxybenzyl)-3H-[1,2,3]triazolo[4,5-d]pyrimidine (159 mg, 478 μmol , crude), (S)-pyrrolidin-3-ol (62.5 mg, 717 μmol), and DIPEA (124 mg, 167 μL , 956 μmol) were combined with CH₃CN (500 μL) in a 5-mL vessel to give a dark-green solution. The reaction mixture was stirred overnight and purified directly by preparative reversed-phase HPLC (column: Gemini 5 μm C₁₈ 110A 75 \times 30 mm; λ = 300 nm; flow rate: 30 mL min⁻¹), eluting with a gradient formed from 0.05% Et₃N in H₂O and CH₃CN (80:20 \rightarrow 5:95 over 8 min). The combined product-containing fractions were evaporated to yield 161 mg (88%) of (S)-1-(5-tert-butyl-3-(4-methoxybenzyl)-3H-[1,2,3]triazolo[4,5-d]pyrimidin-7-yl)pyrrolidin-3-ol (36) as a light-yellow solid. MS (*m/z*): 383.3 [*M* + *H*]⁺; ¹H NMR (400 MHz, CDCl₃): δ = 7.45–7.47 (d, 2H, *J* = 8 Hz), 6.82–6.84 (d, 2H,

$J=8$ Hz), 5.64 (s, 2H), 4.60–4.76 (m, 1H), 4.15–4.54 (m, 2H), 3.82–4.09 (m, 2H), 3.76 (s, 3H), 2.03–2.30 (m, 2H), 1.39 ppm (s, 9H).

c) Synthesis of 39: (S)-1-(5-*tert*-Butyl-3-(4-methoxybenzyl)-3H-[1,2,3]triazolo[4,5-*d*]pyrimidin-7-yl)pyrrolidin-3-ol (**36**) (156 mg, 408 μ mol) and triethylsilane (474 mg, 651 μ L, 4.08 mmol) were combined with TFA (15.0 mL) in a 200-mL flask to give a colorless solution. The reaction mixture was heated at 70 °C and stirred for 22 h. The reaction mixture was concentrated in vacuo to yield (S)-1-(5-*tert*-butyl-3H-[1,2,3]triazolo[4,5-*d*]pyrimidin-7-yl)pyrrolidin-3-yl 2,2,2-trifluoroacetate, which was used crude in the subsequent step. (S)-1-(5-*tert*-Butyl-3H-[1,2,3]triazolo[4,5-*d*]pyrimidin-7-yl)pyrrolidin-3-yl 2,2,2-trifluoroacetate (crude, 52.8 μ mol), 5-(chloromethyl)-1-cyclopropyl-1H-tetrazole (16.8 mg, 106 μ mol), and 1,8-diazabicyclo[5.4.0]undec-7-ene (DBU; 106 μ mol) were combined with *N,N*-dimethylformamide (DMF; 250 μ L) in a 5-mL vessel at room temperature and stirred overnight. CH₃OH (500 μ L) was added to the reaction mixture and stirred at room temperature for 1 h. The reaction mixture was purified directly by preparative reversed-phase HPLC (column: Gemini 5 μ m C₁₈ 110A 75 × 30 mm; λ = 300 nm; flow rate: 30 mL min⁻¹) eluting with a gradient formed from 0.05% Et₃N in H₂O and CH₃CN (80:20 → 5:95 over 8 min). The combined product-containing fractions were evaporated to yield 8.2 mg (40%) of (3S)-1-[5-*tert*-butyl-3-[(1-cyclopropyl)tetrazol-5-yl)methyl]triazolo[4,5-*d*]pyrimidin-7-yl]pyrrolidin-3-ol (**39**) as a light-yellow gum. MS (*m/z*): 385.3 [*M*+*H*]⁺; ¹H NMR (600 MHz, [D₆]DMSO): δ = 6.22 (s, 2H), 5.03–5.17 (d, 1H, *J* = 36 Hz), 4.38–4.57 (d, 1H, *J* = 36 Hz), 3.94–4.31 (m, 3H), 3.62–3.90 (m, 3H), 3.32 (s, 3H), 1.87–2.21 (m, 2H), 1.28 (s, 9H), 1.21–1.26 (m, 2H), 1.06–1.16 ppm (m, 2H); HRMS: (*m/z*) [*M*+*H*]⁺ calcd for C₁₇H₂₄N₁₀O: 384.2134, found: 385.2215.

Animals in research

Animal work was performed according to the Swiss federal law for animal protection and was approved by the Veterinary Office Basel. Animals were provided an acclimation period of >5 days before use, conventional hygienic conditions for housing (temperature: 20–24 °C, minimum relative humidity: 40%, light/dark cycle: 12 h), and standard diet; access to food and drinking water ad libitum. Specific details on permissions can be provided upon request.

Acknowledgements

It is with pleasure that we thank all our collaborators whose contributions made this work possible and so enjoyable, especially Michel Dietz, Olivier Gavelle, Jørgen Nielsen, Didier Pomeranc, Didier Rombach, Astride Schnöbelen, Tanja Minz, Anja Osterwald, Camille Perret, and Elisabeth Zirwes.

Keywords: CB2 receptor agonists • fibrosis • inflammation • lead optimization • triazolopyrimidines

- [1] P. Pacher, R. Mechoulam, *Prog. Lipid Res.* **2011**, *50*, 193–211.
- [2] P. Pacher, P. Mukhopadhyay, R. Mohanraj, G. Godlewski, S. Batkai, G. Kunos, *Hypertension* **2008**, *52*, 601–607.
- [3] A. A. Izzo, K. A. Sharkey, *Pharmacol. Ther.* **2010**, *126*, 21–38.
- [4] a) S. Lotersztajn, F. Teixeira-Clerc, B. Julien, V. Deveaux, Y. Ichigotani, S. Manin, J. Tran-Van-Nhieu, M. Karsak, A. Zimmer, A. Mallat, *Br. J. Pharmacol.* **2008**, *153*, 286–289; b) B. Horváth, L. Magid, P. Mukhopadhyay, S. Batkai, M. Rajesh, O. Park, G. Tanchian, R.-Y. Gao, E. C. Goodfellow, M. Glass, R. Mechoulam, P. Pacher, *Br. J. Pharmacol.* **2012**, *165*, 2462–2478.

- [5] P. Mukhopadhyay, M. Rajesh, H. Pan, V. Patel, B. Mukhopadhyay, S. Batkai, B. Gao, P. Pacher, *Free Radic. Biol. Med.* **2010**, *48*, 457–467.
- [6] P. Pacher, S. Batkai, G. Kunos, *Pharmacol. Rev.* **2006**, *58*, 389–462.
- [7] a) D. Centonze, A. Finazzi-Agro, G. Bernardi, M. Maccarrone, *Trends Pharmacol. Sci.* **2007**, *28*, 180–187; b) J. Fernández-Ruiz, *Br. J. Pharmacol.* **2009**, *156*, 1029–1040.
- [8] B. Hu, H. Doods, R. D. Treede, A. Ceci, *Pain* **2009**, *143*, 206–212.
- [9] P. Anand, G. Whiteside, C. J. Fowler, A. G. Hohmann, *Brain Res. Rev.* **2009**, *60*, 255–266.
- [10] C. J. Fowler, S. B. Gustafsson, S. C. Chung, E. Persson, S. O. Jacobsson, A. Bergh, *Curr. Top. Med. Chem.* **2010**, *10*, 814–827.
- [11] I. Bab, A. Zimmer, E. Melamed, *Ann. Med.* **2009**, *41*, 560–567.
- [12] M. Maccarrone, *Prog. Lipid Res.* **2009**, *48*, 344–354.
- [13] T. Bíró, B. I. Tóth, G. Haskó, R. Paus, P. Pacher, *Trends Pharmacol. Sci.* **2009**, *30*, 411–420.
- [14] R. G. Pertwee, A. C. Howlett, M. E. Abood, S. P. Alexander, V. Di Marzo, M. R. Elphick, P. J. Greasley, H. S. Hansen, G. Kunos, K. Mackie, R. Mechoulam, R. A. Ross, *Pharmacol. Rev.* **2010**, *62*, 588–631.
- [15] R. G. Pertwee, *Handb. Exp. Pharmacol.* **2005**, *168*, 1–51.
- [16] J. W. Huffman, *Mini Rev. Med. Chem.* **2005**, *5*, 641–649.
- [17] a) S. Brogi, F. Corelli, V. Di Marzo, A. Ligresti, C. Mugnaini, S. Pasquini, A. Tafi, *Eur. J. Med. Chem.* **2011**, *46*, 547–555; b) E. J. Gilbert, G. Zhou, M. K. Wong, L. Tong, B. B. Shankar, C. Huang, J. Kelly, B. J. Lavey, S. W. McCombie, L. Chen, R. Rizvi, Y. Dong, Y. Shu, J. A. Kozlowski, N. Y. Shih, R. W. Hipkin, W. Gonsiorek, A. Malikzay, C. A. Lunn, L. Favreau, D. J. Lundell, *Bioorg. Med. Chem. Lett.* **2010**, *20*, 608–611; c) L. Tong, B. B. Shankar, L. Chen, R. Rizvi, J. Kelly, E. Gilbert, C. Huang, D. Y. Yang, J. A. Kozlowski, N. Y. Shih, W. Gonsiorek, R. W. Hipkin, A. Malikzay, C. A. Lunn, D. J. Lundell, *Bioorg. Med. Chem. Lett.* **2010**, *20*, 6785–6789; d) G. A. Thakur, R. Tichkule, S. Bajaj, A. Makriyannis, *Expert Opin. Ther. Pat.* **2009**, *19*, 1647–1673; e) J. H. Lange, M. A. van der Neut, A. J. Borst, M. Yildirim, H. H. van Stuijvenberg, B. J. van Vliet, C. G. Kruse, *Bioorg. Med. Chem. Lett.* **2010**, *20*, 2770–2775; f) C. Mugnaini, S. Nocerino, V. Pedani, S. Pasquini, A. Tafi, M. De Chiaro, L. Bellucci, M. Valoti, F. Guida, L. Luongo, S. Dragoni, A. Ligresti, A. Rosenberg, D. Bolognini, M. G. Cascio, R. G. Pertwee, R. Moaddel, S. Maione, V. Di Marzo, F. Corelli, *Chem. Med. Chem.* **2012**, *7*, 920–934.
- [18] L. A. Matsuda, S. J. Lolait, M. J. Brownstein, A. C. Young, T. I. Bonner, *Nature* **1990**, *346*, 561–564.
- [19] M. Stahl, H. Mauser, *J. Chem. Inf. Mod.* **2005**, *45*, 542–548.
- [20] cAMP assays were performed with CHO cells expressing human CB1 and CB2 receptor variants as described in: C. Ullmer, S. Zoffmann, B. Bohrmann, H. Matile, L. Lindemann, P. J. Flor, P. Malherbe, *Br. J. Pharmacol.* **2012**, *167*, 1448–1466. Efficacies are expressed as percentages relative to 1 μ M CP55940. EC₅₀ values are the average of determinations (*n* = 1) performed in triplicate. Binding data (*K*) generally correlated with the cAMP data for CB1 and CB2.
- [21] β -Arrestin recruitment assays were performed according to the instructions of the manufacturer (DiscoverX, Fremont, CA, USA). Efficacies are expressed as percentages relative to 1 μ M CP55940. Compounds with > 80% efficacy were considered full agonists.
- [22] Q. Liu, A. Makriyannis (University of Connecticut), Int. PCT Pub. No. WO 2003035005 A3, **2003**.
- [23] AlogP: A. K. Ghose, V. N. Viswanadhan, J. J. Wendoloski, *J. Phys. Chem. A* **1998**, *102*, 3762–377224.
- [24] Ligand efficiency: a) C. Abad-Zapatero, J. T. Metz, *Drug Disc. Today* **2005**, *10*, 464–469; b) I. D. Kuntz, K. Chen, K. A. Sharp, P. A. Kollman, *Proc. Natl. Acad. Sci. USA* **1999**, *96*, 9997–10002.
- [25] a) Molecular Operating Environment (MOE) ver. 2014.09, Chemical Computing Group Inc., 1010 Sherbooke Street West, Suite #910, Montreal, QC H3A 2R7 (Canada), **2015**; b) J. Standfuss, P. C. Edwards, A. D'Antona, M. Fransen, G. Xie, D. D. Oprian, G. F. Schertler, *Nature* **2011**, *471*, 656–660.
- [26] Lyophilization solubility assay (LYSA): a high-throughput solubility screening assay that assesses the kinetic solubility of a test compound in phosphate buffer at pH 6.5 from evaporated DMSO compound stock solution.
- [27] The microsomal stability assay measures the rate of disappearance (clearance: CL_{int} [μ L min⁻¹ kg⁻¹]) of a test compound from incubations with liver microsomes from human, rat, or mouse supplemented with metabolic cofactors (typically NADPH). The assay is used primarily for

- early assessment of metabolic stability by ranking relative CYP-mediated metabolism propensities of compounds within chemical series and guiding lead optimization toward sufficiently stable compounds to attain the required pharmacokinetics. L. Di, C. Keefer, D. O. Scott, T. J. Strelevitz, G. Chang, Y.-A. Bi, Y. Lai, J. Duckworth, K. Fenner, M. D. Troutman, R. S. Obach, *Eur. J. Med. Chem.* **2012**, *57*, 441–448.
- [28] Radioligand binding assays were performed with membranes prepared from cells expressing human or mouse CB2 receptors using [³H]CP55940 (PerkinElmer) as radioligand. EC₅₀ or K_i values were calculated from a single experiment using triplicates of ten different compound concentrations.
- [29] The parallel artificial membrane permeability assay (PAMPA) is a method that determines the permeability of substances from a donor compartment through a lipid-infused artificial membrane into an acceptor compartment. M. Kansy, F. Senner, K. Gubernator, *J. Med. Chem.* **1998**, *41*, 1007–1010.
- [30] The thermodynamic solubility assay (THESA) determines the equilibrium solubility of a compound. THESA is a medium-throughput assay that differentiates from other high-throughput solubility tests in that the assay is conducted in customized buffers, and the starting material is a characterized solid sample. Review: C. Saal, A. C. Petereit, *Eur. J. Pharm. Sci.* **2012**, *47*, 589–595.
- [31] FaSSiF/FeSSiF: equilibrium solubility determined for powder dissolved in fasted (FaSSiF) and fed (FeSSiF) simulated intestinal fluids buffers at pH 6.5. Review: P. Augustijns, B. Wuyts, B. Hens, P. Annaert, J. Butler, J. Brouwers, *Eur. J. Pharm. Sci.* **2014**, *57*, 322–332.
- [32] M. L. Howard, J. J. Hill, G. R. Galluppi, M. A. McLean, *Comb. Chem. High Throughput Scr.* **2010**, *13*, 170–187.
- [33] P-glycoprotein (permeability glycoprotein, abbreviated as P-gp) is the most studied and best characterized drug transporter. J. D. Wessler, L. T. Grip, J. Mendell, R. P. Giugliano, *J. Am. Coll. Cardiol.* **2013**, *61*, 2495–2502.
- [34] The GSH assay is the primary tool to assess the potential of reactive metabolite formation of new compounds. Review: a) I. A. Blair, *Curr. Drug Metab.* **2006**, *7*, 853–872. The hERG assay serves to access the potential of a test compound to interfere with the channel and in turn result in undesired side effects at the cardiac system: b) J. W. Warmke, B. Ganetzky, *Proc. Natl. Acad. Sci.* **1994**, *91*, 3438–3442; c) M. C. Sanguinetti, M. Tristani-Firouzi, *Nature* **2006**, *440*, 463–469.
- [35] Cytochrome P450 (CYP) enzymes play a central role in drug metabolism. The potential of a test compound to be metabolized and subsequently excreted is assessed systematically: a) C. Barau, B. Ghaleh, A. Berdeaux, D. Morin, *Fund. Clin. Pharm.* **2015**, *29*, 1–9; b) J. M. McKim in *Encyclopedia of Drug Metabolism and Interactions, Vol. 4* (Ed.: A. V. Lyubimov), Wiley, Chichester, **2012**, pp. 223–250.
- [36] Q. Wei, Z. Dong, *Am. J. Physiol.-Renal. Physiol.* **2012**, *303*, F1487–F1494.
- [37] M. G. Madsen, *Dan. Med. J.* **2013**, *60*, B4582.
- [38] A. C. Ucerro, A. Benito-Martin, M. C. Izquierdo, M. D. Sanchez-Ninö, A. B. Sanz, A. M. Ramos, S. Berzal, M. Ruiz-Ortega, J. Egido, A. Ortiz, *Int. Urol. Nephrol.* **2014**, *46*, 765–776.
- [39] K. Wojcikowski, H. Wohlmuth, D. W. Johnson, G. Gobe, *Phytotherapy Res.* **2010**, *24*, 875–884.

Received: May 18, 2015

Revised: June 23, 2015

Published online on July 21, 2015